Zygote **16** (May), pp. 93–110. © 2008 Cambridge University Press
doi:10.1017/S0967199407004492 Printed in the United Kingdom

Ultrastructural changes in goat interspecies and intraspecies reconstructed early embryos

Yong Tao[1,4], *Lizi Cheng*[1], *Meiling Zhang*[1], *Bin Li*[1], *Jianping Ding*[1], *Yunhai Zhang*[1,3], *Fugui Fang*[1], *Xiaorong Zhang*[1,*] *and Poul Maddox-Hyttel*[3]

Department of Animal Sciences, College of Animal Science and Technology, Anhui Agricultural University, Hefei, China; Department of Genetics and Biotechnology, Faculty of Agricultural Sciences, Aarhus University, Tjelle, Denmark; and Department of Basic Animal and Veterinary Sciences, Anatomy and Cell Biology, Royal Veterinary and Agricultural University, Frederiksberg, Denmark

Date submitted: 4.12.06. Date accepted: 18.04.07

Summary

The low efficiency of somatic cell nuclear transfer may be related to the ultrastructural deviations of reconstructed embryos. The present study investigated ultrastructural differences between *in vivo*-produced and cloned goat embryos, including intra- and interspecies embryos. Goat ear fibroblast cells were used as donors, while the enucleated bovine and goat oocytes matured *in vitro* as recipients. Goat–goat (GG), goat–cattle (GC) and goat *in vivo*-produced embryos at the 2-cell, 4-cell, 8-cell and 16-cell stages were compared using transmission electron microscopy. These results showed that the three types of embryos had a similar tendency for mitochondrial change. Nevertheless, changes in GG embryos were more similar to changes in *in vivo*-produced embryos than were GC embryos, which had more extreme mitochondrial deviation. The results indicate the effects of the cytoplast on mitochondria development. The zona pellucida (ZP) in all three types of embryos became thinner and ZP pores in both GC and GG embryos showed an increased rate of development, especially for GC embryos, while *in vivo*-produced embryos had smooth ZP. The Golgi apparatus (Gi) and rough endoplasmic reticulum (RER) of the two reconstructed embryos became apparent at the 8-cell stage, as was found for *in vivo* embryos. The results showed that the excretion of reconstructed embryos was activated on time. Lipid droplets (LD) of GC and GG embryos became bigger, and congregated. In *in vivo*-produced embryos LD changed little in volume and dispersed gradually from the 4-cell period. The nucleolus of GC and GG embryos changed from electron dense to a fibrillo-granular meshwork at the 16-cell stage, showing that nucleus function in the reconstructed embryos was activated. The broken nuclear envelope and multiple nucleoli in one blastomere illuminated that the nucleus function of reconstructed embryos was partly changed. In addition, at a later stage in GC embryos the nuclear envelope displayed infoldings and the chromatin was concentrated, implying that the blastomeres had an obvious trend towards apoptosis. The gap junctions of the three types of embryos changed differently and GG and GC embryos had bigger perivitelline and intercellular spaces than did *in vivo*-produced embryos. These results are indicative of normal intercellular communication at an early stage, but this became weaker in later stages in reconstructed embryos. In conclusion, inter- and intraspecies reconstructed embryos have a

[*]All correspondence to: Zhang Xiaorong. Faculty of Animal Genetics, Breeding and Reproduction, College of Animal Science and Technology, Anhui Agricultural University, Changjiang West Rd 130, Hefei, 230036, China. Tel: +86 551 5782 488. Fax: +86 551 5785 543. e-mail: zxr@ahau.edu.cn
[1]Faculty of Animal Genetics, Breeding and Reproduction, Department of Animal Sciences, College of Animal Science and Technology, Anhui Agricultural University, Hefei 230036, China.
[2]Section of Population Genetics and Embryology, Department of Genetics and Biotechnology, Faculty of Agricultural Sciences, Aarhus University, Tjelle 8830, Denmark.
[3]Department of Basic Animal and Veterinary Sciences, Anatomy and Cell Biology, Royal Veterinary and Agricultural University, Groennegaardsvej 7, DK-1870 Frederiksberg C, Denmark.
[4]These authors contributed equally to this work.

https://doi.org/10.1017/S0967199407004492 Published online by Cambridge University Press

similar pattern of developmental change to that of *in vivo*-produced embryos for ZP, rough ER, Gi and nucleolus, but differ for mitochondria, LD, vesicles, nucleus and gap junction development. In particular, the interspecies cloned embryos showed more severe destruction. These ultrastructural deviations might contribute to the compromised developmental potential of reconstructed embryos.

Keywords: Embryo, Interspecies somatic cell nuclear transfer, Mitochondria, Ultrastructure, Zona

Introduction

Since the birth of Dolly in 1996 (Wilmut *et al.*, 1997), nuclear transfer technology has developed rapidly, and many offspring from various species have been born. The nuclear transfer embryos, however, show reduced competence resulting in decreased pregnancy and birth rates after transfer when compared with *in vivo*-produced embryos. The reduced competence of nuclear transfer embryos is associated with morphological deviations during bovine prehatching development (Laurincik *et al.*, 2000, 2002; Hyttel *et al.*, 2001; Baran *et al.*, 2002). In these investigations, however, most attention was paid to the nuclear structure and function. Thus, there is a need to focus on the changes in the cytoplasm that have occurred by nuclear transfer.

It is well known that the quality of *in vitro*-produced (IVP) embryos is compromised if compared with *in vivo* embryos living in a physiologically optimal microenvironment. The *in vitro*-fertilized embryos differ ultrastructurally from those produced *in vivo*. For example, *in vitro*-fertilized compact morulae of cattle had a greater volume density of lipid droplets (LD), a reduced proportional volume of total mitochondria, a greater volume density of vacuoles, and an increased cytoplasmic-to-nuclear ratio (Crosier *et al.*, 2000). Moreover, the blastomeres of *in vivo* embryos had a tendency to be rounder up to the 16-cell stage and to form a more compact mass at the morula stage than their IVP counterparts. Some structures (such as microvilli, phagosomes/lysosomes, intercellular junctions and intermediate filaments) appeared or reappeared, while others (such as LD, vesicles with flocculent materials, cortical granules, nuclear annulate lamellae, nuclear envelope blebs) decreased or disappeared. These changes were observed about the time of the 1-cell stage and were later in IVP than in *in vivo* embryos. Other structures present in both IVP and *in vivo* embryos either changed (such as mitochondria, ER, Golgi apparatus and nucleoli) or did not change (cytoplasmic annulate lamellae). Vacuolated nucleoli in both IVP and *in vivo* embryos were observed from the 2-cell stage (Plante & King, 1994). Compared with *in vivo* embryos, IVP embryos had decreased volume densities of cytoplasm, of mitochondria and of nuclei, and increased volume densities of mature mitochondria, nuclei, blastocoele, and apoptotic bodies, proportional volumes of nuclei and inclusion bodies in inner cell mass cells of blastocysts and proportional volume of vacuoles and the volume density of lipid (Crosier *et al.*, 2001). Bovine blastocysts produced *in vitro* possessed deviations in volume densities of organelles associated with cellular metabolism, as well as deviations associated with altered embryonic differentiation (Crosier *et al.*, 2001).

The optimization of the *in vitro* culture system may improve the developmental capacity by improving the ultrastructural features of embryos. For instance, growth hormone (GH) treatment promoted the development of bovine IVP embryos by eliminating glycogen storage in the inner cell mass, stimulating the exocytosis of lipid vesicles of blastocysts, increasing the volume density of embryonic mitochondria, and altering ZP structure and pore size (Sabine *et al.*, 2004). Epidermal growth factor (Makarevich *et al.*, 2005) and heat shock also influenced the embryo ultrastructure (Rivera *et al.*, 2003).

Morphometric analysis offers a more objective method of assessing differences in cellular ultrastructure than may occur in embryos because of nuclear transfer. Interspecies nuclear transfer is an invaluable tool for studying nucleus–cytoplasm interactions, and it provides a possible alternative to clone animals whose oocytes are difficult to obtain (Wen *et al.*, 2003). By now, very few reports have been seen on the ultrastructural change of embryos produced by interspecies nuclear transfer (Hamilton *et al.*, 2004). The objective of the present study was to use morphometric analysis to investigate the ultrastructure of organelles in interspecies cloned embryos at early stage.

Materials and methods

Reagents and chemicals

All chemicals and reagents, unless otherwise specified, were from Sigma. Tissue culture medium 199 (TCM-199), Dulbecco's modified Eagle's medium/nutrient mixture, F12 Ham's (DMEM/F12, 1:1, Gibco-BRL), and M2 medium (M-7167) were used for oocyte *in vitro* maturation and embryo *in vitro* culture. Fetal bovine serum (FBS) used in the study was purchased from Gibco. Follicle-stimulating hormone (FSH) and luteinizing hormone (LH) were purchased from Institute of Zoology, Chinese Academy of Sciences.

https://doi.org/10.1017/S0967199407004492 Published online by Cambridge University Press

Estrogen (E2), hyaluronidase (HAE), cytochalasin B, HEPES and mineral oil.

In vivo embryo production

For production of *in vivo* embryos (multiple ovulations, MO), goat donors were superovulated by intramuscular (i.m.) administration of FSH given in a series of decreasing doses over a 3- or 4-day period. Estrus was induced by i.m. administration of prostaglandin $F_{2\alpha}$ on the morning and evening of the third or fourth day of FSH treatment. The donor goats were inseminated three times after first standing estrus with semen. Embryos used in this study were recovered by surgical uterine flushing on either day 1, 2, 2.5 or 4 after first insemination. The recovered embryos at the 2-cell, 4-cell, 8-cell, and 16-cell stages were identified respectively.

Embryo reconstruction by nuclear transfer

The cloned embryos were reconstructed by using the methods reported previously (Liu *et al.*, 2004; Zhang *et al.*, 2004, 2005). In brief, Boer goat ear skin slices were collected, and then the fibroblast cell line was established. The cumulus and oocyte complexes of goat and cattle were collected from a local slaughterhouse, and then matured *in vitro*. The oocytes at metaphase II were chosen and used as recipients. By micromanipulation, the goat somatic cells were transferred to goat and cattle oocytes respectively. Then, the reconstructed intraspecies or interspecies embryos were obtained by fusion and activation, and then the reconstructed embryos developed to the 2-cell, 4-cell, 8-cell, and 16-cell stages.

Preparation of ultrathin sections

Embedment procedures were modified from Crosier *et al.* (2000) and Hamilton *et al.* (2004). In brief, the embryos at different stages were fixed respectively in 2.5% (v/v) glutaraldehyde (SP1-CHEM) in phosphate-buffered saline (PBS, 0.01 M sodium phosphate, 0.15 M sodium chloride, pH 7.4), and then held at 4 °C until processed for transmission electron microscopy. The embryos were removed from fixative and washed three times for a total of 15 min in 0.1 M PBS. A solution of low-melting-point agarose (4% w/v) was prepared in 0.2 M PBS, and embryos were individually transferred into liquid agarose at 37 °C. The agarose was cooled to 25 °C and allowed to harden. Agarose-embedded embryos were then removed as individual 3 mm^3 blocks with a razor blade. Agarose blocks were postfixed in 1% osmium tetroxide (OsO4, SP1-Chem.) in 0.2 M PBS for 90 min. The samples were washed three times in deionized water for a total of 15 min, subjected to an alcohol dehydration series (30% 10 min, 50% 15 min, 70% 2 h or overnight, 80% 10 min, 95% 15 min, 100% 30 min, 100% 30 min). The embryos were removed to 1,2-epoxypropane (Lingfeng Chemical Co. Ltd) 30 min for transparence, and then transferred to 1,2-epoxypropane and resin Epon812 (1:1) 1.5 h. Samples were individually embedded in 50% Epon812 (Serva), 12% dodecenyl succinic anhydride (DDSA, SP1-Chem.), and 38% nadic methyl anhydride (MNA, SP1-Chem.). Resin blocks were solidified at 45 °C for at 12 h, and 60 °C for at least 48 h. Ultrathin sections (80 nm thick) were prepared from each embryos with an ultrathin section machine (LKB-NUBA, NOVA) and blade (LKB2**178**, knife maker II, BROMMA). The ultrathin sections were placed in Butvar-covered 75-mesh copper grids. Sections were poststained with 1% (w/v) methanolic uranyl acetate (Lanzhou State-owned Factory 404) 5 min, and then 2.66% Reynolds lead citrate (SP1-Chem) 5 min. The sections were rinsed in a stream of distilled water and dried prior to examination. Sections were visualized on a transmission electron microscope (Jeol, JEM-1230). Seven to 10 random micrographs were taken to represent each embryo.

Ultrastructure analysis

Selected organelles and structures were examined: mitochondria, zona pellucida (ZP), Golgi apparatus (Gi), endoplasmic reticulum (ER), lipid droplet (LD), vesicles, lysosomes and the nucleus.

Three types of normal mitochondria were distinguished: (i) mature mitochondria (MM) containing well developed and evenly stacked cristae; (ii) hooded mitochondria (HM), i.e. immature mitochondria having poorly developed, peripheral cristae and a particular hood; and (iii) vacuolated mitochondria (VM) containing a membrane-bound vesicle. The volume densities for the three individual mitochondrial types were added to represent the volume density of total mitochondria (Crosier *et al.*, 2001). Three random embryos at each stage were used. Five random micrographs were taken to count the total number of mitochondria of each embryo. The proportion of HM to MM was calculated, at the same time, the morphologically abnormal mitochondria were counted, and the proportion to the total mitochondria was calculated. Meanwhile, LD diameter was evaluated, and then compared with the mitochondrial diameter. Moreover, the volume density occupied by other cellular components was determined by the point count method using a sampling of five to six random micrographs from each embryos.

Statistical analysis

Data were expressed as mean ± SEM. The frequencies were subjected to arcsine transformation and analysed

https://doi.org/10.1017/S0967199407004492 Published online by Cambridge University Press

by chi-squared test. A p value < 0.05 was considered statistically significant.

Results

Zona pellucida

Three types of embryos differed in the change of surface, pore, perivitelline space (PVS) and thickness of ZP (Fig. 1).

Mitochondria

Three types of normal mitochondria were found in each embryo: HM containing few cristae (Fig. 3*a*), VM with vesicles and cristae (Fig. 3*b*), and MM (Fig. 3*c*). The proportion of HM to mitochondria was calculated for all three types of embryos (Fig. 4). Generally, the rate decreased for all the three types of embryos along with development. For GC embryos, HM rate at 2-cell stage (42.5%) was significantly higher than that of 4-cell (26.4%), 8-cell (27.8%) and 16-cell stages (23.2%) ($p < 0.05$). For GG embryos, the HM rate showed no significant change from the 2- to the 16-cell stage ($p > 0.05$). For *in vivo*-derived embryos, the HM rate at the 2-cell (45.6%) and the 4-cell stages (43.1%) was significantly higher than that at the 16-cell stage (28.7%) ($p < 0.05$). HM rate of GC embryos at the 4-cell stage was significantly lower than that of GG embryos and *in vivo*-derived embryos at the same stage ($p < 0.05$). HM rate of GG embryos had no statistical difference with that of *in vivo*-derived embryos at all stages ($p > 0.05$).

The proportion of MM to total normal mitochondria was calculated for three types of embryos (Fig. 5). Generally, the rate increased for all the three types of embryos along with the development. For GC embryos, MM rate at 16-cell stage (53.6%) was significantly higher than that of the 2-cell stage (40.0%) ($p < 0.05$). MM rate of GC embryos was significantly higher than that of GG embryos at the same respective stages ($p < 0.05$). MM rate of GG embryos had no difference with that of *in vivo*-derived embryos ($p > 0.05$). GG embryos displayed the same change as *in vivo*-derived embryos, while, in GC embryos, the HM were more quickly replaced by MM.

Besides the normal mitochondria, morphologically abnormal mitochondria were also found, more or less, in all the three types of embryos at any stage. Deviations included myelin denaturalization, the matrix coagulation and rupture of membranes (Fig. 6*a–c*). The proportion of morphologically abnormal mitochondria to total mitochondria was examined (Table 1). In GC embryos, this rate was significantly higher at the 8-cell stage (51.5%) that at the 2-cell (31.0%) and the 4-cell stages (38.1%) ($p < 0.05$), but not different from that at the 16-cell stage (42.9%, $p < 0.05$). In GC embryos, the proportion of abnormal mitochondria at the 4-cell, 8-cell, and 16-cell stages was significantly higher than that at the 2-cell stage (20.6%, $p < 0.05$). In contrast, *in vivo*-derived embryos had no significant change in the proportion ($p > 0.05$). GC embryos had a significantly higher proportion of abnormal mitochondria than *in vivo*-derived embryos at the same respective stages ($p < 0.05$), but had no significant difference as compared with GG embryos at 4-cell, 8-cell, and 16-cell stages ($p > 0.05$). GG embryos showed a significantly higher proportions of abnormal mitochondria at the 4-cell, 8-cell, 16-cell stages than *in vivo*-derived embryos at the same stages ($p < 0.05$).

Golgi apparatus

No well developed Gi was found in GC embryos at the 2-cell or the 4-cell stage. In GC the 8-cell embryos, poorly polarized Gi, with no clear secretion side (concave) or mature side (convexity), were distinguished (Fig. 7*a*). At the 16-cell stage, Gi had developed further and had become polarized. The secretion side presented small vesicles of medium electron density and different sizes (Fig. 7*b*). GG embryos had no Gi at the 2-cell or 4-cell stages. In the 8-cell stage, Gi started to form (Fig. 7*c*) and, at the 16-cell stage, Gi developed quickly with increased number and volume (Fig. 7*d*). In *in vivo*-derived embryos, no Gi was observed at the 2-cell and the 4-cell stages. At the 8-cell stage, Gi appeared near the nucleus. The morphology was similar to that seen in the two types of reconstructed embryos (Fig. 7*e*). At the 16-cell stage, the Gi had a typical structure (Fig. 7*f*).

Endoplasmic reticulum

In *in vivo*-derived embryos, some rough ER (RER) appeared at the 8-cell stage (Fig. 8*a*). The RER cisternae became longer at the 16-cell stage. In GG embryos, likewise no RER was found at the 2-cell and 4-cell stages, while a sparse amount was observed at the 8-cell stage (Fig. 8*b*). In GC embryos, again no RER was found at the 2-cell and 4-cell stages, but RER developed abundantly at the 8-cell stage (Fig. 8*c*). The RER cisternae were longer at the 16-cell stage, approaching and connecting to the nuclear envelope (Fig. 8*d*). In summery, RER appeared at the same stage of development for three types of embryos, and the reconstructed embryos had the similar change of structure in RER. The SER was noted in all the three types of embryos at all stages. The electronic density of the SER was almost the same as of the cytoplasmic matrix. Many ribosomes were seen around the nucleus (Fig. 8*d*). The SER was close to Gi, RER, and

https://doi.org/10.1017/S0967199407004492 Published online by Cambridge University Press

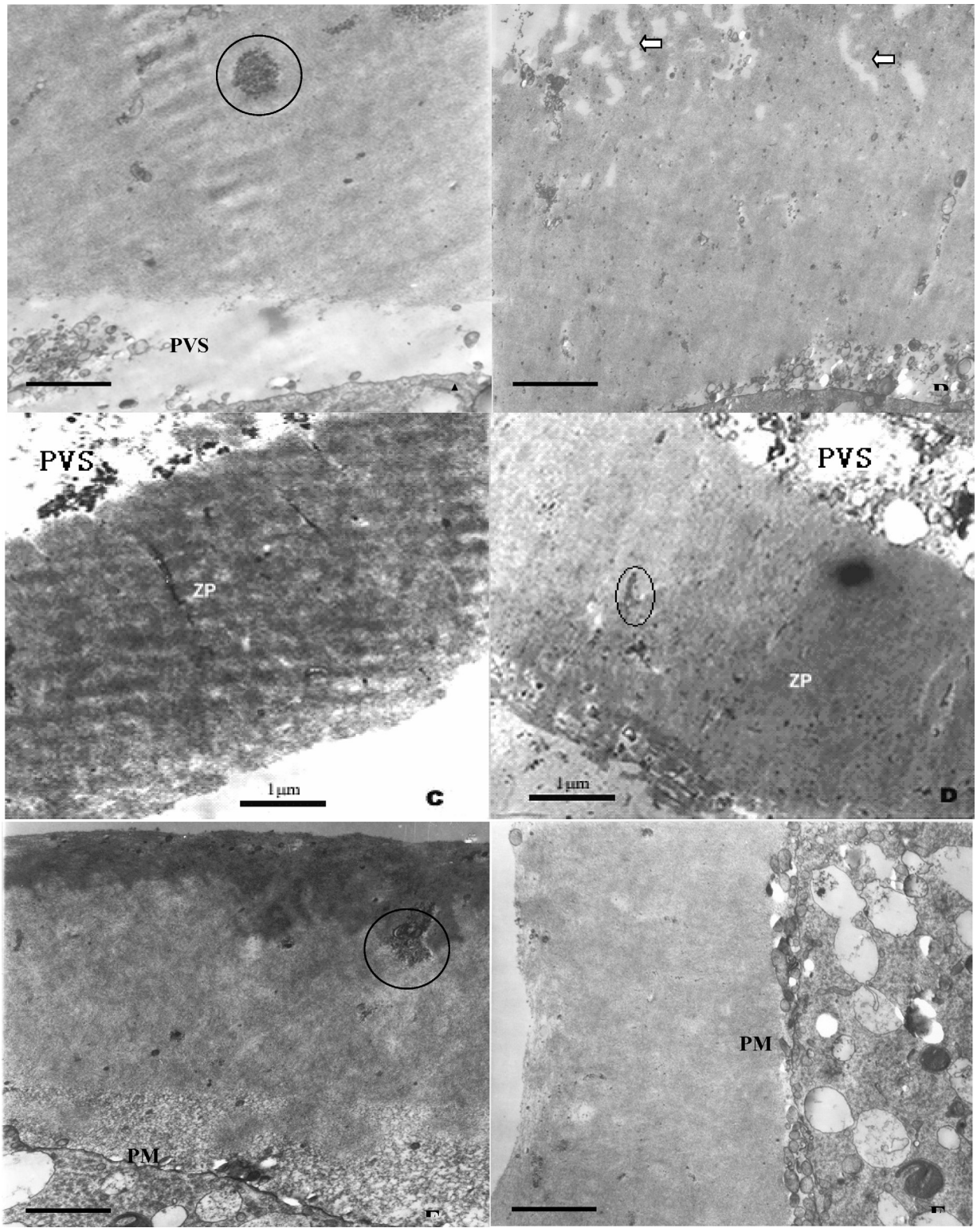


Figure 1 Representative zona pellucida (ZP) morphology of different embryos. (*a*) Goat–cattle reconstructed embryo at the 2-cell stage. (*b*) Goat–cattle reconstructed embryo at the 8-cell stage. (*c*) Goat–goat reconstructed embryo at the 2-cell stage. (*d*) Goat–goat reconstructed embryo at the 8-cell stage. (*e*) Goat *in vivo* fertilized embryos at the 2-cell stage. (*f*) Goat *in vivo* fertilized embryos at the 8-cell stage. The gathering glycogen is shown (circle). The pores in the zona pellucida are shown (arrow). ZP, zona pellucida; PVS, perivitelline space, PM, cytoplasmic membrane. Bar = 1 μm.

https://doi.org/10.1017/S0967199407004492 Published online by Cambridge University Press

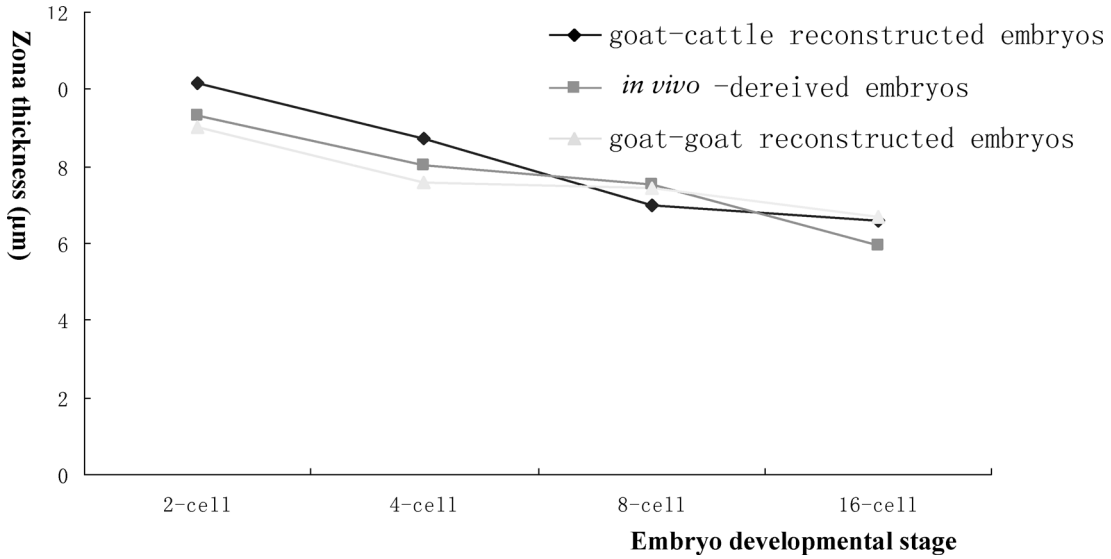


Figure 2 Change of ZP thickness of different embryos. Each value was the mean from photographs ($n = 7$–9) of three embryos. No significant difference was found between the three types of embryo at the same stage ($p < 0.05$).

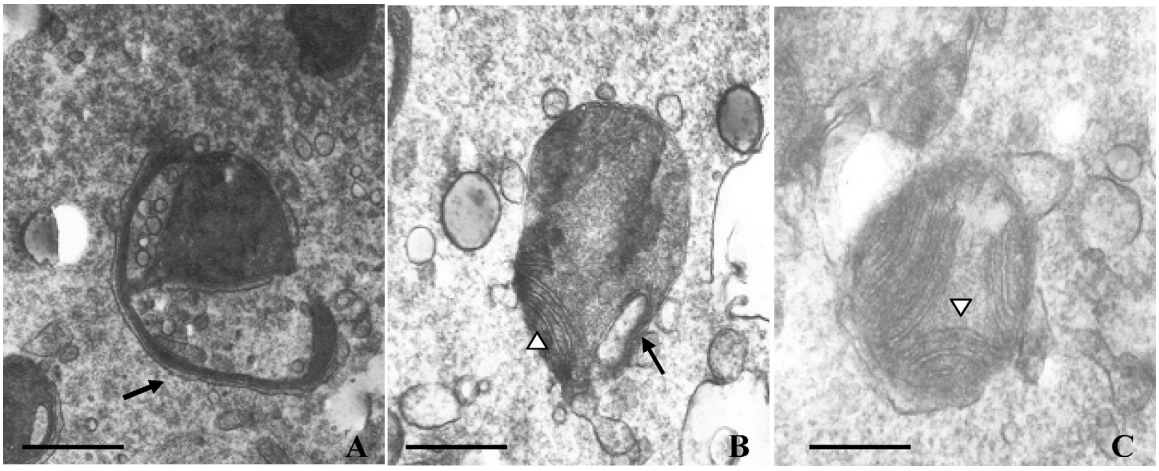


Figure 3 Electron micrographs showing different types of mitochondria. (*a*) Hooded mitochondria (HM) containing few cristae and a typical hood (arrow). (*b*) Vacuolated mitochondria (VM). The vacuole (arrow) and cristae (arrowhead) are shown. (*c*) Mature mitochondria (MM) presenting many cristae (arrowhead). Bar = 200 nm.

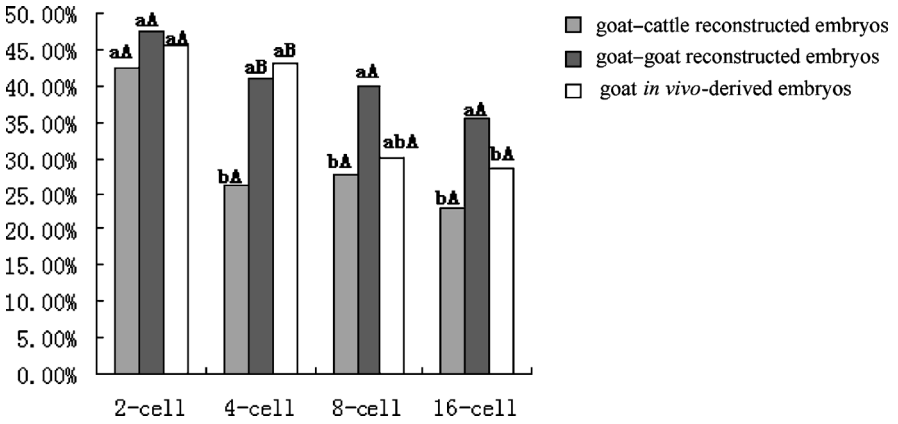


Figure 4 Proportion of hooded mitochondria in different embryos. a,b – Values compared at different stages of the same type of embryos, Groups lacking common letters are significantly different ($p < 0.05$). A,B – Values compared in different types of embryos at the same stage. Groups lacking common letters are significantly different ($p < 0.05$).

https://doi.org/10.1017/S0967199407004492 Published online by Cambridge University Press

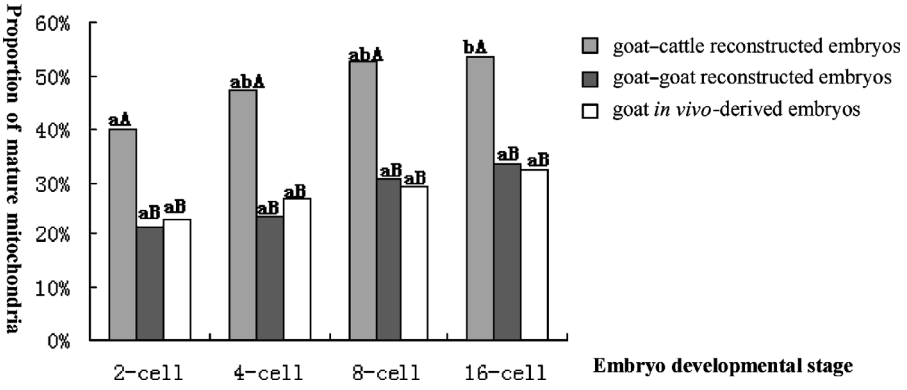


Figure 5 Proportion of mature mitochondria of different embryos. a,b – Values compared at different stages of the same type of embryos, Groups lacking common letters are significantly different ($p < 0.05$). A,B – Values compared in different types of embryos at the same stage. Groups lacking common letters are significantly different ($p < 0.05$).

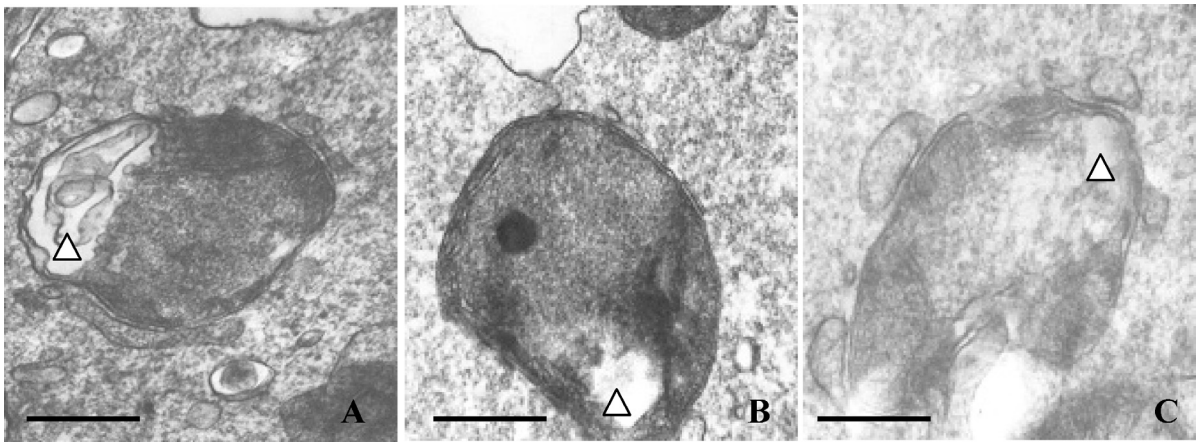


Figure 6 Electron micrographs showing representative morphology of abnormal mitochondria. (*a*) Myelin denaturation. (*b*) Lucent mitochondrial matrix. (*c*) Membrane breakdown, ruptured cristae. The abnormal structures in mitochondria were shown respectively (arrowheads). Bar = 200 nm.

Table 1 Proportion of abnormal mitochondria in different embryos

Embryo genre	2-cell	4-cell	8-cell	16-cell
GC embryos	31.0 (35/113)^{a,c}	38.1 (40/105)^{a,c}	51.5 (51/99)^{b,c}	42.9 (48/112)^{a,b,c}
GG embryos	20.6 (21/102)^{a,d}	47.1 (41/87)^{b,c}	48.0 (49/102)^{b,c}	48.3 (43/89)^{b,c}
In vivo embryos	18.5 (17/92)^{a,d}	18.2 (20/110)^{a,d}	22.2 (24/108)^{a,d}	27.7 (26/94)^{a,d}

^{a,b}Values within the same row lacking common letters are significantly different ($p < 0.05$); ^{c,d}values within the same column lacking common letters are significantly different ($p < 0.05$).

especially mitochondria, and most mitochondria were surrounded by SER (Fig. 8*e*, *f*).

Lipid droplet

In *in vivo*-derived embryos, a few LD gathered at the 2- and 4-cell stages (Fig. 9*a*), but no aggregation was found at 8-cell stage, and most dispersed in the cytoplasm (Fig. 9*b*), while only few LD were observed at 16-cell stage. In GC embryos, aggregated LD were found at the 2-, 4- (Fig. 9)*c*, 8- (Fig. 9*d*) and 16-cell stages, and the degree of aggregation increased gradually, especially after the 4-cell stage. Around the LD, some mitochondria were often found (Fig. 9*c*–*f*). In GG embryos, a few LD gathered at the 2- and 4-cell stages (Fig. 9*e*), and even more at the 8-cell stage (Fig. 9*f*).

The diameter of LDs in the reconstructed embryos began to increase at the 4-cell stage, and reached a peak at the 16-cell stage ($p < 0.05$). The LD diameter in GG embryos at the 8-cell stage was significantly higher than that of GG embryos at the 2-cell stage ($p < 0.05$). In *in vivo*-derived embryos, the LD diameter

https://doi.org/10.1017/S0967199407004492 Published online by Cambridge University Press

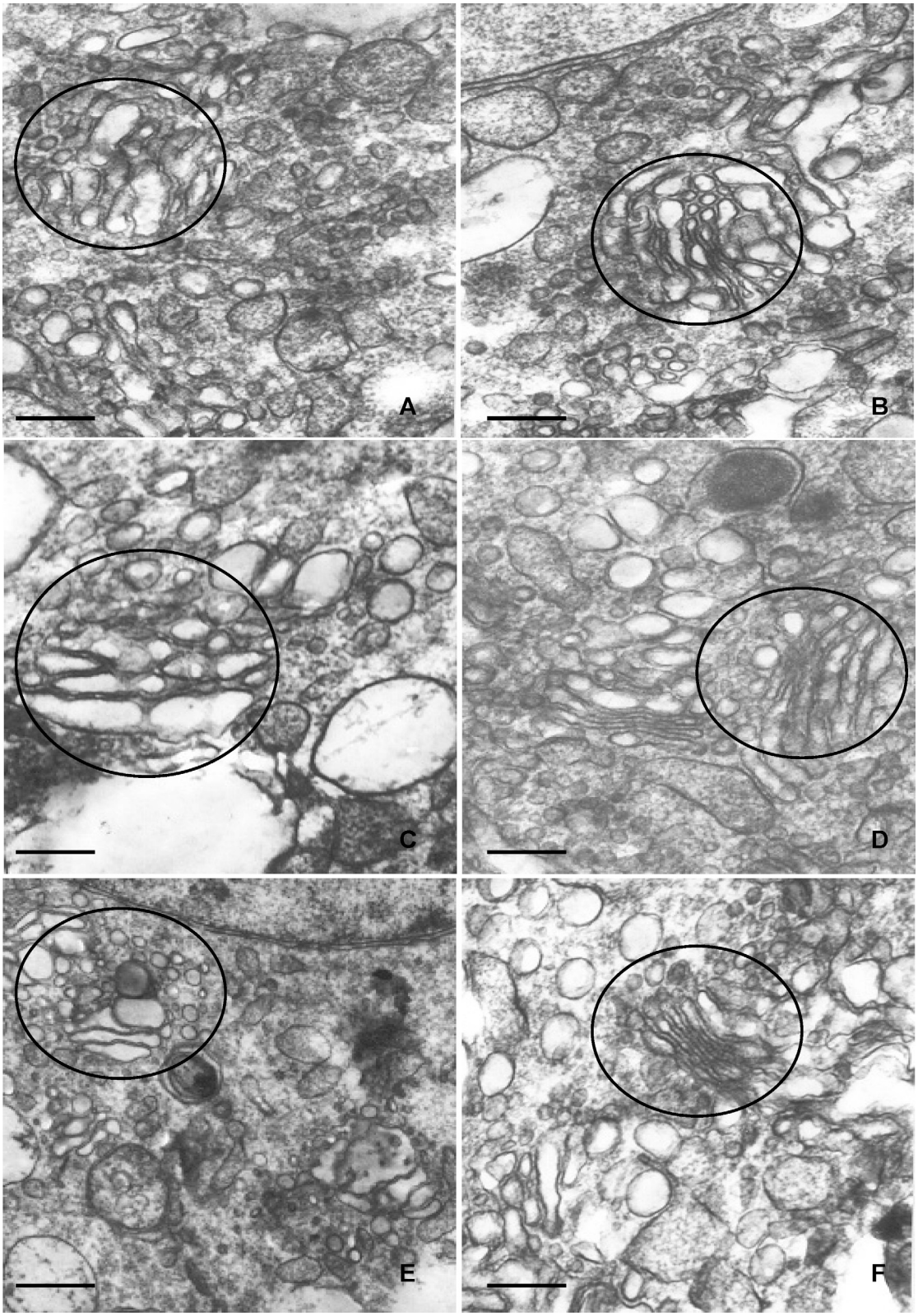


Figure 7 Electron micrographs showing Golgi apparatus. (*a*) Goat–cattle reconstructed 8-cell embryo. (*b*) Goat–cattle reconstructed 16-cell embryo. (*c*) Goat–goat reconstructed 8-cell embryo. (*d*) Goat–goat reconstructed 16-cell embryo. (*e*) *In vivo* fertilized 8-cell embryo. (*f*) *In vivo* fertilized 16-cell embryo. SER, smooth endoplasmic reticulum. Gi, Golgi apparatus. Bar = 500 nm.

https://doi.org/10.1017/S0967199407004492 Published online by Cambridge University Press

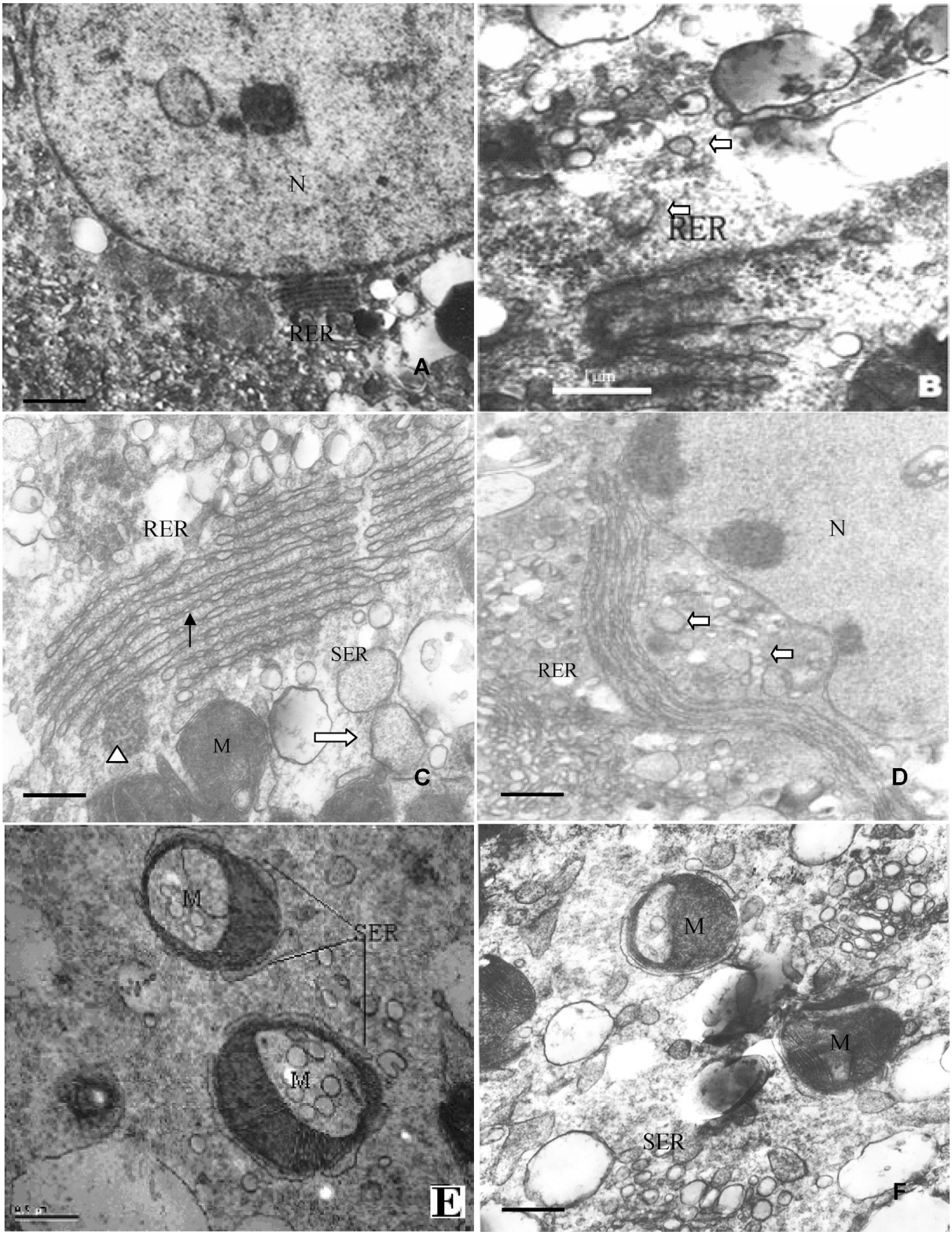


Figure 8 Electron-micrographs showing representative images of endoplasmic reticulum. (*a*) *In vivo* fertilized 8-cell embryo. (*b*) Goat–goat reconstructed 8-cell embryo. (*c*) Goat–cattle 8-cell embryo. (*d*) Goat–cattle reconstructed 16-cell embryo. (*e*,*f*) Representative structure of smooth endoplasmic reticulum (SER). The mitochondria surrounded by SER. RER, rough endoplasmic reticulum; M, mitochondria; N, nucleus. Long and thin arrows showed the gathering ribosomes. Thick and empty arrows showed RER. Triangle arrows indicate the aggregated ribosomes. Bars = 1 μm.

https://doi.org/10.1017/S0967199407004492 Published online by Cambridge University Press

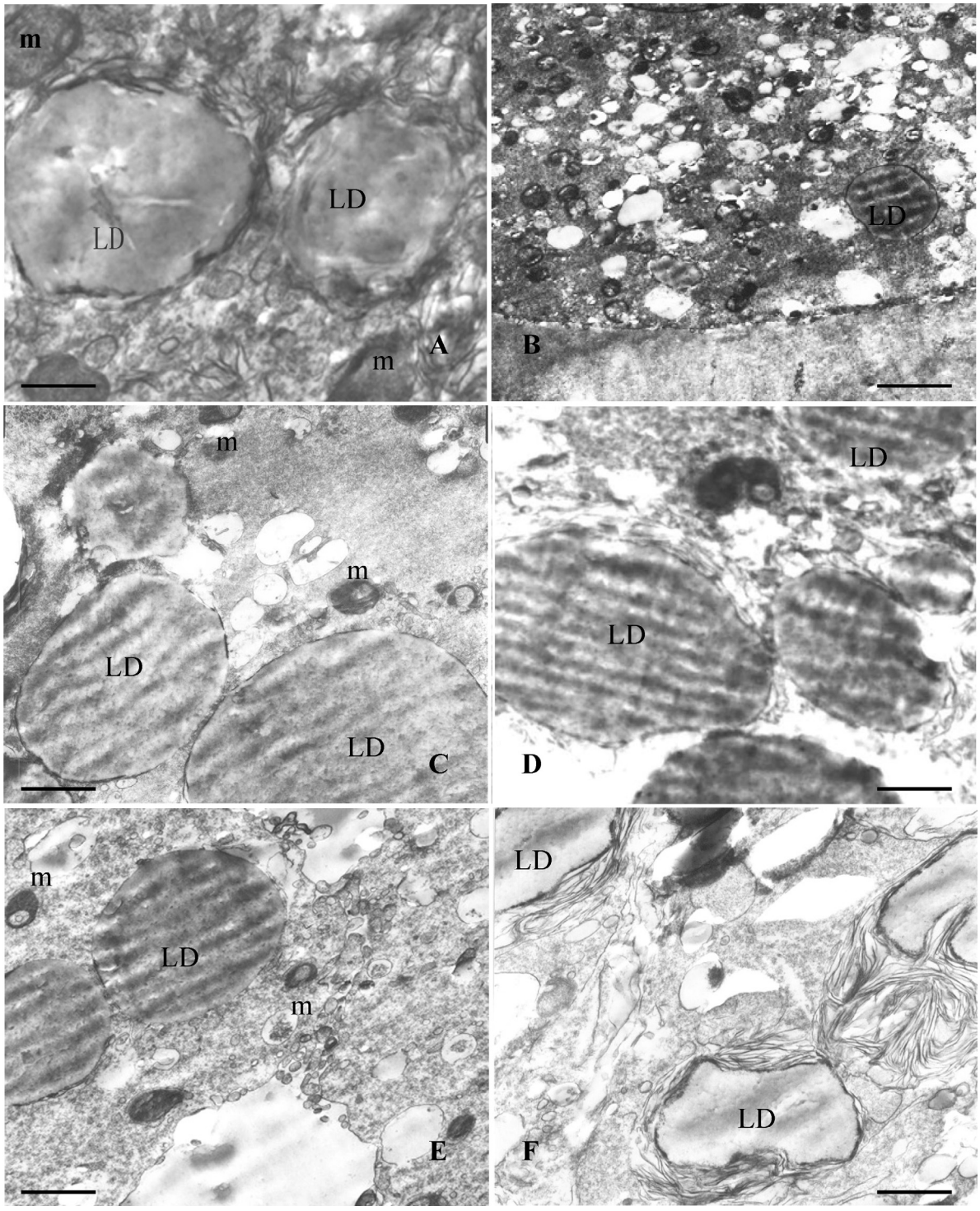


Figure 9 Electron-micrographs showing lipid droplets. (*a*) Goat *in vivo*-fertilized 4-cell embryo. (*b*) Goat *in vivo*-fertilized 8-cell embryo. (*c*) Goat–goat reconstructed 4-cell embryo. (*d*) Goat–goat reconstructed 8-cell embryo. (*e*) Goat–cattle reconstructed 4-cell embryo. (*f*) Goat–cattle reconstructed 8-cell embryo. LD, Lipid droplet; m, mitochondria. Bar = 400 nm.

also tended to increase with development, though not statistically significant ($p > 0.05$). GC embryos at the 4-, 8-, and 16-cell stages had significantly higher LD diameter than *in vivo*-derived embryos respectively ($p < 0.05$). GG embryos at the 8- and 16-cell stages had significantly higher LD diameter than those in *in vivo*-derived embryos at the same stages ($p < 0.05$) (Table 2). In summary, the lipid content of reconstructed

https://doi.org/10.1017/S0967199407004492 Published online by Cambridge University Press

Table 2 Lipid droplet diameter change in different embryos

Embryos	2-cell (μm)	4-cell (μm)	8-cell (μm)	16-cell (μm)
Goat *in vivo* fertilized	$1.234 \pm 0.129^{a,d}$	$1.802 \pm 0.453^{a,e}$	$2.17 \pm 0.532^{a,e}$	$2.226 \pm 0.597^{a,e}$
Goat–cattle reconstructed	$1.347 \pm 0.241^{a,d}$	$2.785 \pm 1.125^{b,d}$	$3.316 \pm 1.983^{b,d}$	$6.721 \pm 2.535^{c,d}$
Goat–goat reconstructed	$1.365 \pm 0.265^{a,d}$	$1.772 \pm 0.527^{a,b,e}$	$2.511 \pm 0.923^{b,d}$	$5.624 \pm 1.226^{c,d}$

$^{a-c}$Values within the same row lacking common letters are significantly different ($p < 0.05$); ^{d,e}values within the same column lacking common letters are significantly different ($p < 0.05$).

Table 3 Ratio of lipid droplet diameter to mitochondria diameter of different embryos

Developmental stage	2-cell	4-cell	8-cell	16-cell
Goat *in vivo* fertilized embryo	1–2	2–3	2–4	3–4
Goat–cattle reconstructed embryo	2–3	2–7	2–9	5–10
Goat–goat reconstructed embryo	2–3	2–4	2–5	5–8

embryos was increased, and this phenomenon was particularly pronounced in interspecies-reconstructed embryos. The ratio of LD diameter to mitochondria diameter increased for all three types of embryos, but this increase was steeper in GC embryos, especially from the 8-cell stage (Table 3).

Lysosome

Lysosomes were found in *in vivo*-derived embryos at the 2-, 4-, 8-, and 16-cell stages without apparent change in number (Fig. 10*a*). In GC embryos, only a few lysosomes were observed at the 2-cell stage, while more were found at the 4-cell stage. In GG embryos, only a few lysosomes were found at the 2-cell stage, while more were observed at the 4-cell stage. A great number of sublysosomes, precursors of lysosomes, were found at the 8-cell stage, and some of these were found with some organelles licked up, as for the mitochondria with abnormal morphology (Fig. 10*b*,*c*).

Vesicle

In *in vivo*-derived embryos, numerous electron-lucent vesicles were found at the 2-, 4-, 8- (Fig. 11*a*) and 16-cell stages, and they distributed uniformally in the cytoplasm. Some vesicles contained some flocculent material. The nucleus was surrounded by small vesicles while the more peripheral vesicles were larger. In GG embryos, a medium number of vesicles were found at the 2-cell stage, distributed equally throughout the cytoplasm. At the 4-cell stage, much more vesicles were observed, and the distribution had become uneven. Some blastomeres contained few vesicles, while others presented numerous aggregated vesicles (Fig. 11*b*). Many vesicles were still found at the 8- and 16-cell stages. In GC embryos, the number of the vesicles did not change much from the 2-cell to 8-cell stage. At the 16-cell stage, more vesicles were found (Fig. 11*c*).

Nucleus

In *in vivo*-derived embryos, the nucleus was round at the 2-, 4- and 8-cell stages, and typically it contained

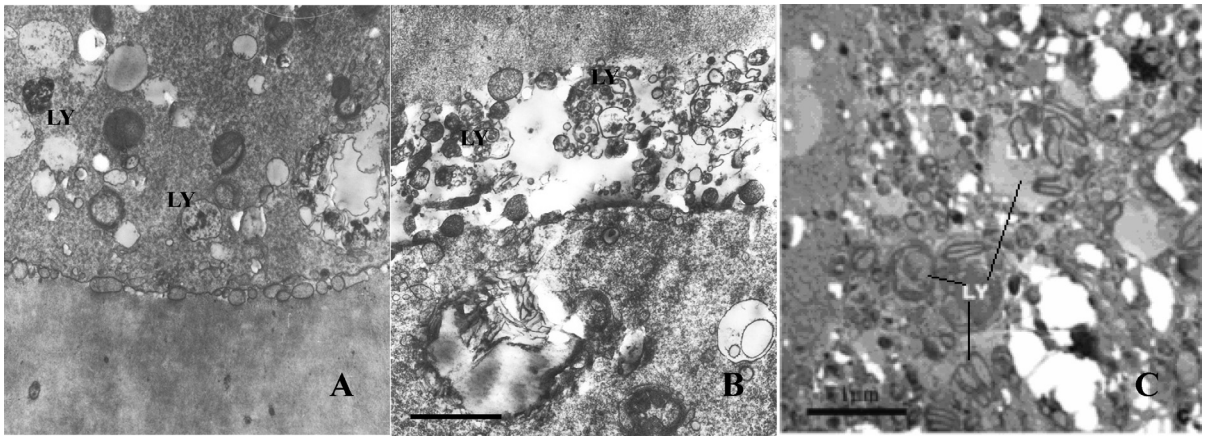


Figure 10 Electron-micrographs showing lysosomes. (*a*) Goat *in vivo*-fertilized 8-cell embryo. A few lysosomes are contained. (*b*) Goat–cattle reconstructed 8-cell embryo. Many lysosomes are contained in perivitelline space (PVS). (*c*) Goat–goat reconstructed 8-cell embryo. Many lysosomes are contained with the abnormal mitochondria. LY, lysosomes; LD, lipid droplet; M, mitochondria; ZP, zona pellucida. Bar = 1 μm.

https://doi.org/10.1017/S0967199407004492 Published online by Cambridge University Press

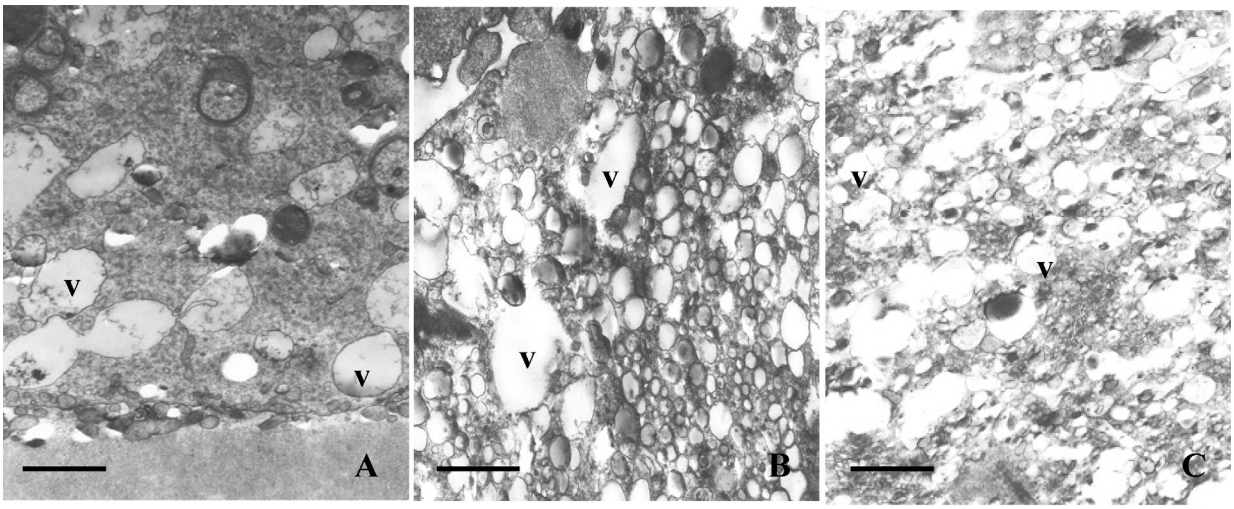


Figure 11 Electron-micrographs showing representative images of the vesicles. (*a*) Goat *in vivo*-fertilized 8-cell embryo. The vesicles have membrane. (*b*) Goat–goat reconstructed 4-cell embryo. Some vesicles have no membrane. (*c*) Goat–cattle reconstructed 16-cell embryo. V, vesicle. Bar = 1 μm.

one or more electron-dense nucleolus precursor bodies (Fig. 12*a*). At the 16-cell stage, the nucleus precursor bodies developed vacuoles and apparently active ribosome-synthesizing fibrillo-granular nucleoli were observed (Fig. 12*b*). In some GC embryos, the nuclear envelope was incomplete exposing the karyoplasm to the cytoplasm (Fig. 12*c*). At the 16-cell stage, the blastomeres had irregularly shaped nuclei, and the nuclear envelope was clearly defined, but undulating (Fig. 12*d*,*f*). In GG embryos, the nuclei were comparable to those of the GC embryos. Occasionally, blastomeres binucleated (Fig. 12*e*).

Membrane and gap junctions

The plasma membrane of the blastomeres in all three types of embryos was intact. However, the membrane of the reconstructed embryos displayed more undulations. The blastomeres were covered by microvilli (Fig. 13*a*, *b*). In *in vivo*-derived embryos, the microvilli extended from the membrane at the 2-cell stage (Fig. 14*a*). At the 8-cell stage, there was no apparent intracellular space (Fig. 14*b*). At the 16-cell stage, the blastomeres contacted each other closely without intercellular spaces (Fig. 14*c*). In GC embryos, the space between blastomeres was considerable from before the 8-cell stage. At the 8-cell stage, the microvilli was quite long (Fig. 14*d*,*e*). At the 16-cell stage, the increasing blastomeres approached to each other, but quite a bit space between the blastomeres was still observed (Fig. 14*f*). In GG embryos, the junction became looser with a small space from the 2- to 8-cell stages (Fig. 14*g*,*h*). At the 16-cell stage, the blastomeres kept nearer (Fig. 14*i*).

Discussion

At present, much more can be deduced from embryo morphology than previously thought and embryo morphology assessment has been one of the most popular methods for embryo selection (Abe *et al.*, 2002a; van Soom *et al.*, 2003). In addition, the ultrastructural features may reflect various physiological anomalies and even apoptosis (Kerr *et al.*, 1994; Desai *et al.*, 2000). Embryos produced by nuclear transfer have a greater variance in morphology and developmental rate. This study found that the intraspecies- and interspecies-reconstructed embryos showed some ultrastructural deviations in organelles, including mitochondria, lysosomes, vesicles, lipid drops and intracellular junctions. These changes may contribute to the reduction in potential viability that is found with reconstructed embryos.

Zona pellucida

The ZP thickness decreases during embryo development and, therefore, this feature may be applied as a useful marker to evaluate, and even predicate, the embryo quality in many species (Cohen *et al.*, 1988; Gabrielsen *et al.*, 2000), including humans (Dirnfeld *et al.*, 2003; Pelletier *et al.*, 2004). It was thought that the fact that the *in vivo* embryo ZP became thinner was related to the oviduct and uterus endoenvironment (Funahashi *et al.*, 2000). Furthermore, that the decrease in ZP thickness was necessary for hatching and implantation at a subsequent time for both *in vivo* and *in vitro* embryos. It was reported that the ZP of *in vitro* fertilized bovine embryos was thinner than that of *in vivo* embryos at the same stages (Abe *et al.*, 1999).

https://doi.org/10.1017/S0967199407004492 Published online by Cambridge University Press

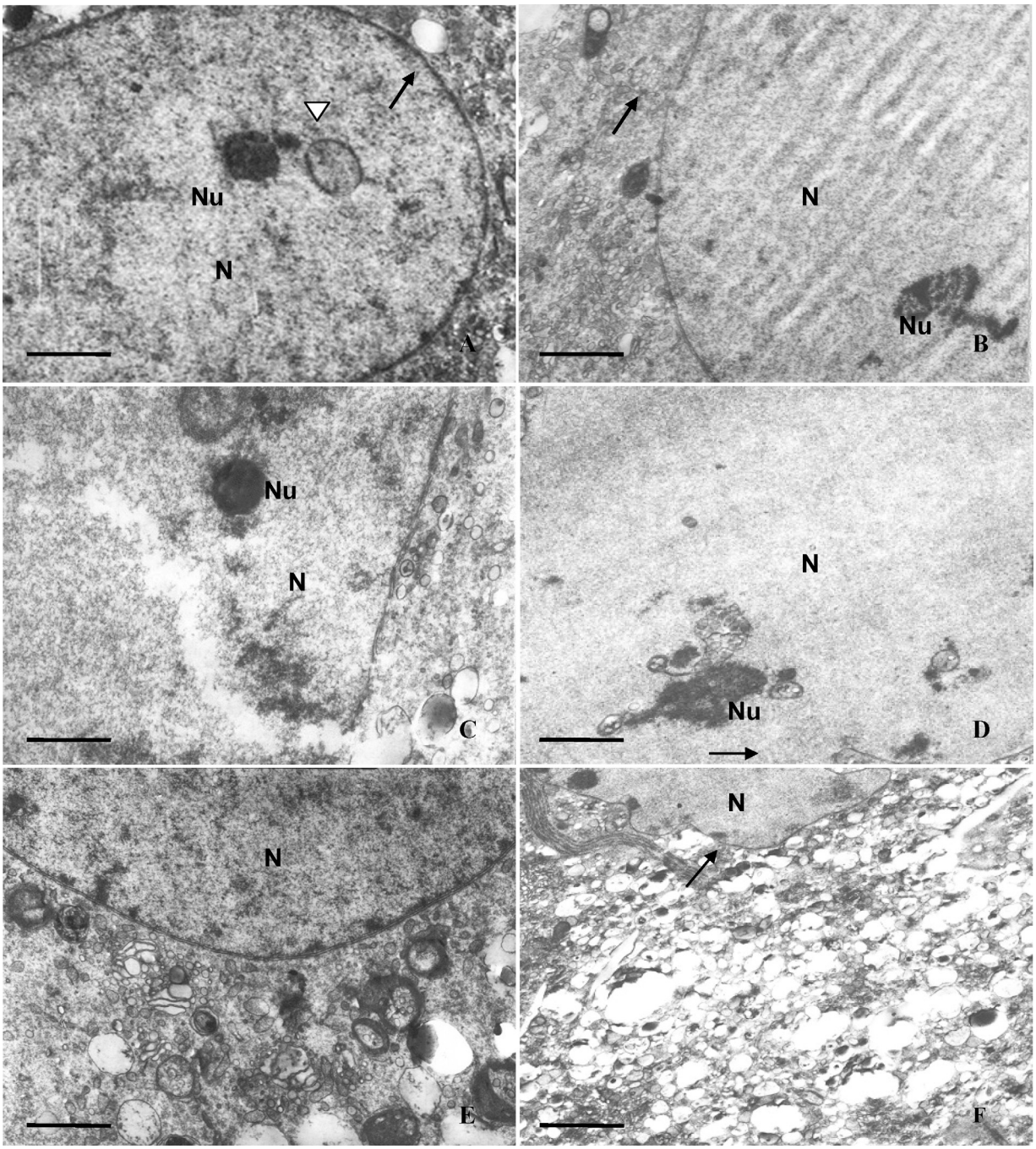


Figure 12 Electron-micrographs showing representative nucleus images. (*a*) Goat *in vivo*-fertilized 8-cell embryo with integrated nuclear envelope and dense nucleolus (Nu). (*b*) Goat *in vivo*-fertilized 8-cell embryo with integrated nuclear envelope and meshwork nucleolus. (*c*) Goat–cattle reconstructed 8-cell embryo with dense nucleolus. The broken nuclear envelope is shown. (*d*) Goat–cattle reconstructed 16-cell embryo with meshwork nucleus, nuclear envelope infolding. (*e*) Goat–goat reconstructed 4-cell embryo containing two nuclei with integrated nuclear envelope. (*f*) Goat-cattle reconstructed 16-cell embryo. N, nucleus (N), arrow shows nuclear envelope. The concentrated chromatin is shown (arrow). Bar = 500 nm.

In addition, the diameter of bovine IVP blastocysts was also increased. We found the similar results in relation to ZP thickness and all three types of embryos became thinner with development, but no statistically significant difference in thickness was found among embryos at the same stage. However, the change in ZP thickness in the GG embryo was more comparable to that of *in vivo* embryos. Our results also showed that, compared with *in vivo* embryos, the ZP of intraspecies cloned embryos was less compact, with more pores and a less smooth surface. This change was more obvious for the ZP of interspecies cloned embryos,

https://doi.org/10.1017/S0967199407004492 Published online by Cambridge University Press

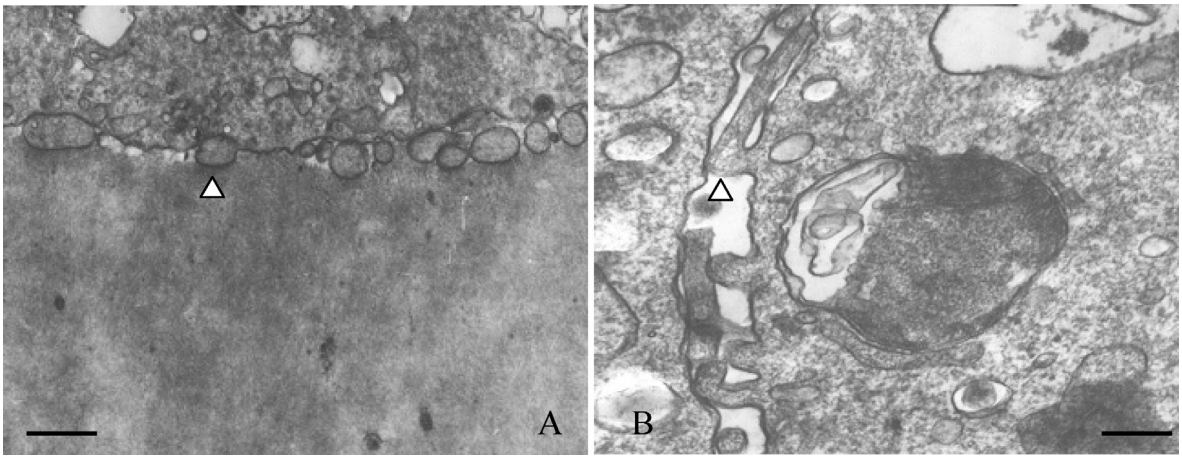


Figure 13 Electron micrographs showing representative microvilli morphology. (*a*) Goat *in vivo*-fertilized 8-cell embryo with short microvilli (Mi). Scale bar, 400 nm. (*b*) Goat–cattle reconstructed 8–cell embryo with long microvilli. Scale bar, 200 nm. The Mi is shown with triangle arrow.

and this finding was identical to previous reports for IVP embryos. (Vanroose *et al.*, 2000; Sabine *et al.*, 2004; Nottola *et al.*, 2005). We speculated that these findings might be indicative of an altered ZP composition.

Mitochondria

The change for mitochondria is the important clue to the embryo's developmental potential. Immature mitochondria are found typically at the early cleavage and morula stages (Sun *et al.*, 1994; Yang *et al.*, 2003), while vacuolated mitochondria are associated with degeneration and subsequent cell death (Enders *et al.*, 1982). With embryo development, the cristae in mitochondria increased (Betteridge, 1988). At the early developmental stage, hooded mitochondria control energy production (Devreker and Englert, 2000), however the IVP embryos have differences (Crosier *et al.*, 2000, 2001). It seems that the development microenvironment of embryos might contribute to their reduced developmental ability. Our study showed that the interspecies and intraspecies cloned embryos and *in vivo*-produced goat embryos had a similar tendency for developmental mitochondria change. However, the change in the GG embryos was more comparable to that in *in vivo* embryos than in the GC embryos, in which the mitochondria had more severe alterations. In this sense, interspecies nuclear transfer is more difficult than previously thought and, therefore, to achieve offspring is more complicated. This difficulty might be due to the homogeneity between the cytoplasm and nucleus. The homogenous cytoplasm could facilitate cooperation and reprogramming to the nucleus, while the hexogenous cytoplasm showed a weaker capacity. Interestingly, mtDNA heteroplasmy in cloned cattle has been reported (Steinborn *et al.*, 2000), while for Dolly there was a lack of heteroplasmy (Evans *et al.*, 1999). Despite being authentic nuclear clones they were, in fact, genetic chimaeras that contained somatic cell-derived nuclear DNA but oocyte-derived mtDNA (Evans *et al.*, 1999). Accordingly, mitochondrial morphological change can be used as an index to evaluate embryo quality and this change might be an indication for improvements in nuclear transfer and in the *in vitro* culture system.

Golgi apparatus and endoplasmic reticulum

This study showed that the three types of embryos had a similar tendency for changes in Gi and in ER. It seems that nuclear transfer causes no apparent injury to the Gi and ER, which indicates that the cloned embryos may have a normal material shipping and secretion model, at least to some extent.

Lipid droplet

Lipid is generally considered the resource for embryo energy and the base for material for membrane structure synthesis. A previous report in cattle found that the blastomeres of IVP embryos had more LD than was found in *in vivo* embryos (Abe *et al.*, 1999). Our study found that the both intra- and interspecies reconstructed embryos had many LD. The volume of these LD increased as development progressed and there was a tendency to aggregate. LD existence is related to the *in vitro* culture system (Monika *et al.*, 2002; Pereira *et al.*, 2005). The *in vitro* culture system used in the present study consisted of 10% fetal bovine serum (FBS), which contributed partly to the LD existence. The study in bovine embryos found that the increase in LD might not be due to active absorption of nutrients from the medium and but instead because the embryos failed to adjust to *in vitro* culture conditions. Therefore, membrane structural change and the lipid accumulation occurred after lipid had been accessed (Crosier *et al.*, 2001). Another report proposed that the

https://doi.org/10.1017/S0967199407004492 Published online by Cambridge University Press

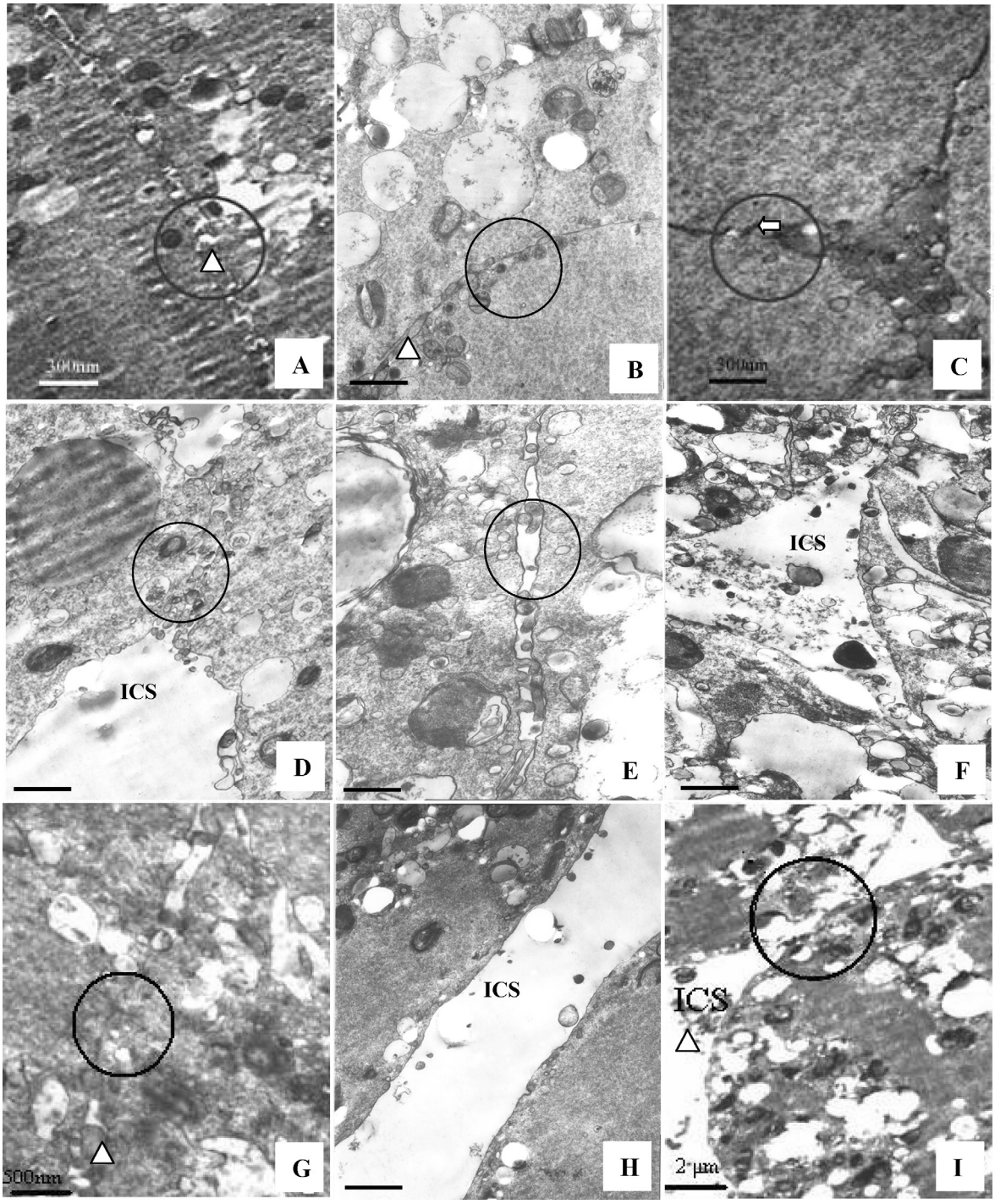


Figure 14 Electron micrographs showing junctions within the blastomeres. (*a*) Goat *in vivo*-fertilized 2-cell embryo with a microvilli (Mi) enchased junction. (*b*) Goat *in vivo*-fertilized 8-cell embryo with gap junction. Bar = 1 µm. (*c*) Goat *in vivo*-fertilized 16-cell embryo with a gap junction. (*d*) Goat–cattle reconstructed 2-cell embryo with a few Mi enchased junctions. Bar = 1 µm. (*e*) Goat–cattle reconstructed 8-cell embryo with a large intercellular space. Bar = 300 nm. (*f*) Goat–cattle reconstructed 16-cell embryo, has loose junction and large intercellular space. Bar = 300 nm. (*g*) Goat–goat reconstructed 2-cell embryo with gap junctions and a Mi enchased junction. (*h*) Goat–goat reconstructed 8-cell embryo contains few Mi and large ICS with no junctions. Bar = 1µm. (*i*) Goat–goat reconstructed 16-cell embryo has a few gap junctions and a large intercellular space. ICS, intercellular space. Arrow heads shows the microvilli, thick and empty arrows show the desmosomes, and the circle shows the junctions.

https://doi.org/10.1017/S0967199407004492 Published online by Cambridge University Press

accumulation of cytoplasmic droplets was due to a reduced cryotolerance (Abe *et al.*, 2002b).

Lipid metabolism is closely related to mitochondria and therefore the relationship of LD rate to mitochondria volume was investigated in the present study. We found that this rate changed little for *in vivo*-produced goat embryos, but that the rate for reconstructed embryos, especially for the interspecies cloned embryos, increased. This lipid accumulation delayed embryo development and decreased blastomere numbers (Thompson *et al.*, 2000). Lipid accumulation was an indication of metabolic reduction in the mitochondria. In other words, the reconstructed embryos had weaker metabolic capacities than was found in *in vivo*-produced embryos. The increase in abnormal mitochondria, as noted above, might also contribute to the accumulation of LD. Furthermore, the accumulated LD might destroy the function of mitochondrial enzymes, so that lipids could not metabolized properly (Campos *et al.*, 1993; Dalakas *et al.*, 1994). We used bovine oocytes that contain many lipids to produce interspecies embryos and we speculated, even though there was a similarity to goat oocytes, that the use of a different cytoplasm donor might be related to the aberration due to heteroplasmy.

Lysosome

A previous study found that the blastomeres of bovine IVP morulae contained few lysosome-like structures (Abe *et al.*, 1999). We found that *in vivo*-produced embryos had few lysosomes and this number changed little with development. In contrast, lysosomes of cloned embryos increased from the 4-cell stage and more residues and secondary lysosome-containing organelles were found in the extracelluar space and PVS. Such a change might be related to *in vitro* culture. The nutrient ingredients in the medium are delivered to the blastomeres firstly through vesicles by pinocytosis and endocytosis and subsequently these vacuoles merge with lysosomes and their contents are digested by hydrolases located in lysosomes. We speculate that addition of serum and the increase in abnormal mitochondria might, in part, cause a lysosome increase to counteract this impact, as some mitochondria were found in lysosomes. This is a kind of compensation and self-recovery. Some articles ingested failed to be digested and formed residues to extrude to PVS and externally out of embryo via the ZP. Consequently, there was an increase in ZP pores, as noted above.

Vesicle

Vesicle formation might be linked to cell ingestion and, therefore, the number of vesicles reflects the absorptive ability of the cell to its environment. Vesicles, in themselves, are not detrimental to the embryo developmental potential and, on the contrary, they play an important role in molecular transportation. Human *in vivo* embryos were found to have an abundant number of vesicles (Pereda & Croxatto 1978; Pereda *et al.*, 1989). We found that *in vivo*-produced embryos had middle-sized vesicles distributed evenly in the blastomeres and that most vesicles were covered by a single membrane. In intraspecies embryos, the vesicles were distributed unevenly in blastomere cytoplasm and some blastomeres were vacuolated, without any cytoplasm and organelles. Interspecies embryos had also vesicle aggregation at a later stage, with reduced cytoplasm and organelles. Cytoplasm vacuolation is one of the indicators of death of a cell. It seems that these vesicles differ from those found in *in vivo*-produced embryos and were abnormal. The increased number of these abnormal vesicles reduced the number and function of other organelles, and, consequently, the cell's metabolism might be influenced negatively. This finding might be an alternative explanation for the compromised developmental capacity and pregnancy rate of cloned embryos.

Nucleus

The nucleus is the centre for controlling heredity and metabolism and is of the great importance to organelles. The nuclei of human *in vivo* embryos have been found to have extensive blebbing of the nuclear envelope (Pereda and Croxatto 1978). In addition, it has been reported that, in cloned embryos, the changes in nucleolar morphology were delayed in bovine somatic nucleotransferred embryos when compared with the embryonic cloned embryos (Baran *et al.*, 2002). Our study showed that the three types of embryos contained a compact nucleolus before the 8-cell stage, similar to that found in human and ovine embryos. The nucleus from the somatic donor was reticulated after nuclear transfer, indicating re-programming, which is related to RNA synthesis. It has been reported that RNA synthesis is launched at the 4-cell stage with the reticulated nucleolus after blastomeres from bovine morulae were transferred to enucleated recipient oocytes (Smith *et al.*, 1996). The proper activation of the nucleolus can avoid developmental arrest. We found that interspecies embryos at the 16-cell stage became reticulated in the nucleolus, indicating the activation of the zygote genome; the abnormal morphology, however, might impair this function.

Cellular membrane and junction

It has been reported there are distinct desmosome-like structures and junctional complex between blastomeres of *in vivo*-produced human embryos (Pereda & Croxatto, 1978; Pereda & Coppo, 1987). In marsupials, the cell–zona adhesion of dunnart *in vivo*

https://doi.org/10.1017/S0967199407004492 Published online by Cambridge University Press

embryos was established at the zygote stage, while cell–cell adhesion was first apparent at the 16-cell stage (Kress & Selwood, 2004). In bovine IVP blastocysts, blastomeres had less well developed junctional complexes and less apical microvilli (Abe *et al*., 1999). In the present study, we found that the *in vivo*-produced goat embryos had an integral membrane, but, in the interspecies embryos, the space between the blastomeres was considerable, the touch area between blastomeres was small and some blastomeres had smooth surfaces without microvilli extrusion. This abnormality might impair the transfer of information between blastomeres.

Discussion

The interspecies and intraspecies reconstructed embryos have similar development changes in the ZP, rough ER, Gi and nucleolus when compared with *in vivo*-produced embryos. Mature mitochondria in reconstructed embryos, especially interspecies cloned embryos, increased more quickly than that of *in vivo*-produced embryos and the number of abnormal mitochondria was higher than *in vivo*-produced embryos. Interspecies embryos have more severe lipid accumulation, broken nuclear envelopes and more nuclei, which is related to apoptosis or abnormal cleavage. Compared with *in vivo*-produced embryos, the reconstructed embryos have larger spaces between blastomeres.

Acknowledgements

We acknowledge the fund support from Anhui Distinguished Youth Sci-tech Project (grant number 06041081) Eleventh Five-Year Sci-tech Project (grant number 06013051A), National Education Department Project (5030001) and International Cooperation Project (Guoke WaiHan 2002-101 and 2004-117). The authors are also grateful to Dr Sun Qingyuan for his great help in manuscript preparation.

References

Abe, H., Otoi, T., Tachikawa, S., Yamashita, S., Satoh, T. & Hoshi, H. (1999). Fine structure of bovine morulae and blastocysts *in vivo* and *in vitro*. *Anat. Embryol*. **199**, 519–27.

Abe, H., Matsuzaki, S. & Hoshi, H. (2002a). Ultrastructural differences in bovine morulae classified as high and low qualities by morphological evaluation. *Theriogenology* **57**, 1273–83.

Abe, H., Yamashita, S., Satoh, T. & Hoshi, H. (2002b). Accumulation of cytoplasmic droplets in bovine embryos and cryotolerance of embryos developed in different culture systems using serum free or serum-containing media. *Mol. Reprod.* **61**, 57–66.

Au, H.K., Yeh, T.S., Kao, S.H., Tzeng, C.R. & Hsieh, R.H. (2005). Abnormal mitochondrial structure in human unfertilized oocytes and arrested embryos. *Ann. New York Acad. Sci.* **1042**, 177–85.

Baran, V., Vignon, X., LeBourhis, D., Renard, J.P. & Flechon, J.E. (2002). Nucleolar changes in bovine nucleotransferred embryos. *Biol. Reprod.* **66**, 534–43.

Betteridge, K.J. (1988). The anatomy and physiology of pre-attachment bovine embryos. *Theriogenology* **29**, 155–87.

Brogliatti, G.M., Palasz, A.T., Rodriguez-Martinez, H., Mapletoft, R.J. & Adams, G.P. (2000). Transvaginal collection and ultrastructure of llama (*Lama glama*) oocytes. *Theriogenology* **54**, 1269–79.

Campos, Y., Huertas, R. & Bautista, J. (1993). Muscle carnitine deficiency and lipid storage myopathy in patients with mitochondrial myopathy. *Muscle Nerve* **16**, 778–81.

Cohen, J., Malter, M., Fehilly, C., Wright, G., Elsner, C., Kort, H. & Massey, J. (1988). Implantation of embryos after partial opening of oocyte zona pellucida to facilitate sperm penetration. *Lancet* **2**, 162.

Crosier, A.E., Farin, Dykstra, M.J., Alexander, J.E. & Farin, C.E. (2000). Ultrastructural morphometry of bovine compact morulae produced *in vivo* or *in vitro*. *Biol. Reprod*. **62**, 1459–65.

Crosier, A.E., Farin, P.W., Dykstra, M.J., Alexander, J.E. & Farin, C.E. (2001). Ultrastructural morphometry of bovine blastocysts produced *in vivo* and *in vitro*. *Biol. Reprod*. **64**, 1375–85.

Dalakas, M.C., Leon-Monzon, M.E. & Bernardini, I. (1994). Zidovudine induced mitochondrial myopathy is associated with muscle calmitine deficiency and lipid storage. *Ann Neurol*. **35**, 482–7.

de Loos, F., van Vliet, C., van Maurik, P. & Kruip, T.A. (1989). Morphology of immature bovine oocytes. *Gamete Res*. **24**, 197–204.

Desai, N.N., Goldstein, J., Rowland, D.Y. & Goldfarb, J.M. (2000). Morphological evaluation of human embryos and derivation of an embryo quality, scoring system specific for day 3 embryos. A preliminary study. *Hum. Reprod.* **15**, 2190–6.

Devreker, F. & Englert, Y. (2000). *In vitro* development and metabolism of the human embryo up to the blastocyst stage. *Eur. J. Obstet. Gynecol. Reprod. Biol*. **92**, 51–6.

Dirnfeld, M., Shiloh, H., Bider, D., Harari, E., Koifman, M., Lahav-Baratz, S. & Abramovici, H. (2003). A prospective randomized controlled study of the effect of short coincubation of gametes during insemination on zona pellucida thickness. *Gynecol. Endocrinol.* **17**, 397–403.

Enders, A.C., Hendricks, A.G. & Binkerd, P.E. (1982). Abnormal development of blastocysts and blastomeres in the rhesus monkey. *Biol. Reprod.* **26**, 353–66.

Evans, M.J., Gurer, C., Loike, J.D., Wilmut, I., Schnieke, A.E. & Schon, E.A. (1999). Mitochondrial DNA genotypes in nuclear transfer-derived cloned sheep. *Nat. Genet.* **23**, 90–3.

Funahashi, H., Ekwall, H. & Rodriguez, M.H. (2000). Zona reaction in porcine oocytes fertilized *in vivo* and *in vitro* as seen with scanning electron microscopy. *Biol. Reprod*. **63**, 1437–2.

Gabrielsen, A., Bhatnager, P.R. & Petersen, K. (2000). Influence of zona pellucida thickness of human embryos on

https://doi.org/10.1017/S0967199407004492 Published online by Cambridge University Press

clinical pregnancy outcome following *in vitro* fertilization treatment. *J. Assist. Reprod. Genet.* **17**, 323–8.

Hamilton, H.M., Peura, T., Laurincik, J., Walker, S.K., Maddocks, S. & Maddox-Hyttel, P. (2004). Ovine cytoplasm directs initial nucleolar assembly in embryos cloned from ovine, bovine, and porcine cells. *Mol. Reprod. Dev.* **69**, 117–25.

Hyttel, P., Laurincik, J., Zakhartchenko, V., Stojkovic, M., Wolf, E., Müller, M., Ochs, R.L. & Brem, G. (2001). Nucleolar protein allocation and ultrastructure in bovine embryos produced by nuclear transfer from embryonic cells. *Cloning* **3**, 69–81.

Kerr, J.F., Winterford, C.M. & Harmon, B.V. (1994). Apoptosis, its significance in cancer and cancer therapy. *Cancer* **73**, 2013–26.

Kress, A. & Selwood, L. (2004). Precedence of cell–zona adhesion over cell–cell adhesion during marsupial blastocyst formation prohibits morula formation and ensures that both the pluriblast and trophoblast are superficial. *Cells Tissues Organs* **177**, 87–103.

Laurincik, J., Zakhartchenko, V., Avery, B., Stojkovic, M., Brem, G., Wolf, W., Miiller, M. & Hyttel, P. (2000). Activation of ribosomal RNA in pre-implantation *in vitro*-produced and nuclear transfer bovine embryos. *Reprod. Domest. Anim.* **35**, 255–9.

Laurincik, J., Zakhartchenko, V., Stojkovic, M., Brem, G., Wolf, E., Müller, M., Ochs, R.L., & Maddox-Hyttel, P. (2002). Nucleolar protein allocation and ultrastructure in bovine embryos produced by nuclear transfer from granulosa cells. *Mol. Reprod. Dev.* **61**, 477–87.

Liptau, H. & Viebahn, C. (1999). Expression patterns of gap junctional proteins connexin 32 and 43 suggest new communication compartments in the gastrulating rabbit embryo. *Differentiation* **65**, 209–19.

Liu, Y., Zhang, X.R., Chen, D.Y., Zhang, Y.H., Zhang, Z.G., Jin, R.T., Wang, C.L., Zhang, M.L., Li, D.W., Li, B., Zhao, H. & Cheng, L.Z. (2004). Study on development of cloned embryo using bovine somatic cell and rabbit oocyte *in vitro*. *Sci. Agric. Sinica.* **37**, 441–5.

Makarevich, A.V., Chrenek, P., Zilka, N., Pivko, J. & Bulla, J. (2005). Preimplantation development and viability of *in vitro* cultured rabbit embryos derived from *in vivo* fertilized gene-microinjected eggs: apoptosis and ultrastructure analyses. *Zygote* **13**, 125–37.

Monika, O., Schernthaner, W., Sinowatz, F. & Wolf, E. (2002). Effects of bovine serum albumin and estrous cow serum on development and ultrastructure of *in vitro*-produced porcine embryos. *Anat. Histol. Embryol*. **31**, 151–7.

Nottola, S.A., Makabe, S., Stallone, T., Familiari, G., Correr, S. & Macchiarelli, G. (2005). Surface morphology of the zona pellucida surrounding human blastocysts obtained after *in vitro* fertilization. *Arch. Histol. Cytol*. **68**, 133–41.

Pelletier, C., Keefe, D.L. & Trimarchi, J.R. (2004). Noninvasive polarized light microscopy quantitatively distinguishes the multilaminar structure of the zona pellucida of living human eggs and embryos. *Fertil. Steril.* **81**, 850–6.

Pereda, J., Cheviakoff, S. C. & Roxatto, H.B. (1989). Ultrastructure of a 4-cell human *embryo* developed *in vivo*. *Hum. Reprod*. **4**, 680–8.

Pereda, J. & Coppo, M. (1987). Ultrastructure of a two-cell human embryo. *Anat. Embryol.* **177**, 91–6.

Pereda, J. & Croxatto, H.B. (1978). Ultrastructure of a seven-cell human embryo. *Biol. Reprod.* **18**, 481–9.

Pereira, D.C., Dode, M.A. & Rumpf, R. (2005). Evaluation of different culture systems on the *in vitro* production of bovine embryos. *Theriogenology* **63**, 1131–41.

Plante, L. & King, W.A. (1994). Light and electron microscopic analysis of bovine embryos derived by *in vitro* and *in vivo* fertilization. *J. Assist. Reprod. Genet*. **11**, 515–29.

Rivera, R.M., Kelley, K.L., Erdos, G.W. & Hansen, P.J. (2003). Alterations in ultrastructural morphology of two-cell bovine embryos produced *in vitro* and *in vivo* following a physiologically relevant heat shock. *Biol. Reprod*. **69**, 2068–77.

Sabine, K., Miodrag, S., Sven, R., Horst-Dieter, R., Eckhard, W. & Fred, S. (2004). Effects of growth hormone on the ultrastructure of bovine preimplantation embryos. *Cell Tissue Res*. **317**, 101–8.

Smith, S.D., Soloy, E. & Kanka, J. (1996). Influence of recipient cytoplasm cell stage on transcription in bovine nucleus transfer embryos. *Mol. Reprod. Dev.* **45**, 444–50.

Steinborn, R., Schinogl, P., Zakhartchenko, V., Achmann, R., Schernthaner, W., Stojkovic, M., Wolf, E., Muller, M. & Brem, G. (2000). Mitochondrial DNA heteroplasmy in cloned cattle produced by fetal and adult cell cloning. *Nat. Genet.* **25**, 255–7.

Sun, Q.Y., Tan, J.H., Qin, P.C. & Yang, Q.Z. (1994). An ultrastructural study on 8–16 cell sheep embryos. *J. Northeast. Agric. Uni.* (in Chinese) **25**, 380–4.

Thompson, J.G. (2000). *In vitro* culture and embryo metabolism of cattle and sheep embryos—a decade of achievement. *Anim. Reprod. Sci*. **61**, 263–75.

Van Soom, A., Mateusen, B., Leroy, J. & de Kruif, A. (2003). Assessment of mammalian *embryo* quality: what can we learn from *embryo* morphology? *Reprod. Biomed. Online* **7**, 664–70.

Vanroose, G., Nauwynck, H., Soom, A.V., Ysebaert, M.T., Charlier, G., Oostveldt, P.V. & de Kruif, A. (2000). Structural aspects of the zona pellucida of *in vitro*-produced bovine embryos: a scanning electron and confocal laser scanning microscopic study. *Biol. Reprod*. **62**, 463–9.

Wen, D., Yang, C., Cheng, Y., Li, J., Liu, Z., Sun, Q., Zhang, J., Lei, L., Wu, Y., Kou, Z. & Chen, D. (2003). Comparison of developmental capacity for intra- and interspecies cloned cat (*Felis catus*) embryos. *Mol. Reprod. Dev.* **66**, 38–45.

Wilmut, I., Schnieke, A.E., McWhir, J., Kind, A.J. & Campbell, K.H. (1997). Viable offspring derived from fetal and adult mammalian cells. *Nature* **385**, 810–3.

Yang, D.S., Liu, D.J., Qi, M.G. & Shorgan, B. (2003). Ultrastructure of *in vitro* produced bovine embryos cultured in two conventional media. *Acta. Veterinaria. Et. Zootechnica. Sinica*. (in Chinese) **34**, 54–8.

Zhang, X.R. & Liu, Y. (2004). Effect of some factors on the fusion rate of bovine–rabbit interspecies reconstructed eggs. *Chin. J. Agric. Biotechnol* **1**, 135–8.

Zhang, Z.G., Zhang, X.R., Liu, Y., Jin, R.T., Wang, C.L., Zhao, H., Li, B., Cao, C.C., Li, D.W. & Cheng, L.Z. (2005). Serial nuclear transfer of goat–rabbit interspecies reconstructed embryos. *Agric. Sci. Chin.* **4**, 629–33.

https://doi.org/10.1017/S0967199407004492 Published online by Cambridge University Press